Kinetic properties of the sodium–calcium exchanger in rat brain synaptosomes

Giovanni Fontana, Robert S. Rogowski and Mordecai P. Blaustein *

Department of Physiology, University of Maryland School of Medicine, Baltimore, MD 21201, USA

1. The kinetic properties of the internal Na^+ (Na_i^+)-dependent $^{45}Ca^{2+}$ influx and external Na^+ (Na_o^+)-dependent $^{45}Ca^{2+}$ efflux were determined in isolated rat brain nerve terminals (synaptosomes) under conditions in which the concentrations of internal Na^+ ($[Na^+]_i$), external Na^+ ($[Na^+]_o$), external Ca^{2+} ($[Ca^{2+}]_o$), and external K^+ ($[K^+]_o$) were varied. Both fluxes are manifestations of Na^+–Ca^{2+} exchange.

2. Ca^{2+} uptake was augmented by raising $[Na^+]_i$ and/or lowering $[Na^+]_o$. The increase in Ca^{2+} uptake induced by removing external Na^+ was, in most instances, quantitatively equal to the Na_i^+-dependent Ca^{2+} uptake.

3. The Na_i^+-dependent Ca^{2+} uptake (measured at 1 s) was activated with an apparent half-maximal $[Ca^{2+}]_o$ ($K_{Ca(o)}$) of about 0·23 mM. External Na^+ inhibited the uptake in a non-competitive manner: increasing $[Na^+]_o$ from 4·7 to 96 mM reduced the maximal Na_i^+-dependent Ca^{2+} uptake but did not affect $K_{Ca(o)}$.

4. The inhibition of Ca^{2+} uptake by Na_o^+ was proportional to $([Na^+]_o)^2$, and had a Hill coefficient (n_H) of ~2·0. The mean apparent half-maximal $[Na^+]_o$ for inhibition ($\bar{K}_{I(Na)}$) was about 60 mM, and was independent of $[Ca^{2+}]_o$ between 0·1 and 1·2 mM; this, too, is indicative of non-competitive inhibition.

5. Low concentrations of alkali metal ions (M^+) in the medium, including Na^+, stimulated the Na_i^+-dependent uptake. The external Na^+ and K^+ concentrations required for apparent half-maximal activation ($K_{M(Na)}$ and $K_{M(K)}$, respectively) were 0·12 and 0·10 mM. Thus, the relationship between Ca^{2+} uptake and $[Na^+]_o$ was biphasic: uptake was stimulated by $[Na^+]_o \leqslant 10$ mM, and inhibited by higher $[Na^+]_o$.

6. The calculated maximal Na_i^+-dependent Ca^{2+} uptake (J_{max}) was about 1530 pmol (mg protein)$^{-1}$ s^{-1} at 30 °C at saturating $[Ca^{2+}]_o$ and external M^+ concentration ($[M^+]_o$), and with negligible inhibition by external Na^+.

7. Internal Na^+ activated the Ca^{2+} uptake with an apparent half-maximal concentration ($K_{Na(i)}$) of about 20 mM and a Hill coefficient, n_H, of ~ 3·0.

8. The J_{max} for the Na_o^+-dependent efflux of Ca^{2+} from $^{45}Ca^{2+}$-loaded synaptosomes treated with carbonyl cyanide *p*-trifluoromethoxy-phenylhydrazone (FCCP) and caffeine (to release stored Ca^{2+} and raise the internal Ca^{2+} concentration ($[Ca^{2+}]_i$) was about 1800–2000 pmol (mg protein)$^{-1}$ s^{-1} at 37 °C.

9. When the membrane potential (V_m) was reduced (depolarized) by increasing $[K^+]_o$, the Na_i^+-dependent Ca^{2+} influx increased, and the Na_o^+-dependent Ca^{2+} efflux declined. Both fluxes changed about 2-fold per 60 mV change in V_m. This voltage sensitivity corresponds to the movement of one elementary charge through about 60% of the membrane electric field. The symmetry suggests that the voltage-sensitive step is reversible.

10. The J_{max} values for both Ca^{2+} influx and efflux correspond to a Na^+–Ca^{2+} exchange-mediated flux of about 425–575 μmol Ca^{2+} (l cell water)$^{-1}$ s^{-1} or a turnover of about one quarter of the total synaptosome Ca^{2+} in 1 s. We conclude that the Na^+–Ca^{2+} exchanger may contribute to Ca^{2+} entry during nerve terminal depolarization; it is likely to be a major mechanism mediating Ca^{2+} extrusion during subsequent repolarization and recovery.

* To whom correspondence should be addressed.

Calcium ions have many important functions in neurons, including a key role in triggering neurotransmitter release at nerve terminals. Much of this trigger Ca^{2+} comes from the extracellular fluid and enters the terminals via voltage-gated Ca^{2+} channels during depolarization (Katz, 1969).

During recovery following neuronal activation, the entering Ca^{2+} must be extruded in order to maintain a steady Ca^{2+} balance even when the neurons fire at a rapid rate for long periods of time. Several mechanisms participate in the removal of Ca^{2+} from the release sites and in the regulation of the cytosolic free Ca^{2+} concentration, $[Ca^{2+}]_i$. These mechanisms include: (1) Ca^{2+} buffering by cytoplasmic proteins (e.g. Andressen, Blümcke & Celio, 1993); (2) Ca^{2+} sequestration in the endoplasmic reticulum (via a calmodulin-insensitive, ATP-driven Ca^{2+} pump; Blaustein, Ratzlaff, Kendrick & Schweitzer, 1978; McGraw, Somlyo & Blaustein, 1980), and in mitochondria (Werth & Thayer, 1994; but see Rasgado-Flores & Blaustein, 1987); and (3) Ca^{2+} extrusion across the plasmalemma via a calmodulin-sensitive ATP-driven Ca^{2+} pump (Gill, Grollman & Kohn, 1981) and via a Na^+–Ca^{2+} exchanger (Sanchez-Armass & Blaustein, 1987). Ca^{2+} buffering and sequestration may be the main mechanisms for rapidly removing Ca^{2+} from the transmitter-releasing sites (Blaustein, 1988), and Na^+–Ca^{2+} exchange may be the primary mechanism by which the Ca^{2+} is extruded from the terminals and Ca^{2+} balance is restored (Sanchez-Armass & Blaustein, 1987; Blaustein, 1988).

Na^+–Ca^{2+} exchanger molecules are present at high concentration in presynaptic nerve terminals (Luther, Yip, Bloch, Ambesi, Lindenmayer & Blaustein, 1992). These molecules cross-react with antibodies raised against dog heart Na^+–Ca^{2+} exchanger, and appear to have a similar molecular structure to the cardiac exchanger molecules (Yip, Blaustein & Philipson, 1992; Furman, Cook, Kasir & Rahamimoff, 1993; Marlier, Zheng, Tang & Grayson, 1993). The kinetics and voltage sensitivity of the mammalian heart Na^+–Ca^{2+} exchanger have been extensively investigated (e.g. Reeves & Sutko, 1983; Miura & Kimura, 1989; Crespo, Grantham & Cannell, 1990; Khananshvili, 1991; Matsuoka & Hilgemann, 1992; Niggli & Lederer, 1993). The aim of the study described here was to explore these properties of the exchanger in isolated nerve terminals (synaptosomes) from rat brain, and to compare the properties of the brain and heart Na^+–Ca^{2+} exchangers. To this end, we measured internal Na^+ (Na_i^+)-dependent $^{45}Ca^{2+}$ influxes and external Na^+ (Na_o^+)-dependent $^{45}Ca^{2+}$ effluxes in synaptosomes during brief (1 s) incubations. These new data address some controversies about the exchanger kinetics, and especially about the interactions between alkali metal ions and Ca^{2+}.

METHODS

Preparation of synaptosomes

Synaptosomes were prepared from the forebrains of adult female Sprague–Dawley rats (175–200 g) as described by Raiteri, Bonnano, Marchi & Maura (1984) and Fontana & Blaustein (1993). Briefly, rats were killed by decapitation and the forebrains were homogenized in forty volumes of 0·32 M sucrose with 10 mM Hepes (pH 7·4 with NaOH). The homogenate was centrifuged at 1000 *g* (5 min, 0–4 °C) to remove nuclei and other dense particles; synaptosomes were isolated from the supernatant by centrifugation at 12000 *g* for 20 min. The buffy layer of pelleted synaptosomes was resuspended by gentle agitation (leaving behind the hard, red mitochondrial pellet) in standard physiological salt solution (Na-PSS).

Solution composition

The Na-PSS contained (mM): 145 NaCl, 2·6 KCl, 2·4 KH_2PO_4, 0·2 $CaCl_2$, 1·2 $MgCl_2$, 10 glucose and 10 Hepes; pH was adjusted to 7·4 with NaOH. The ionic composition of the solutions was varied in most experiments. For example, in low-Na^+ solutions, Na^+ was replaced isosmotically by Li^+ (Li-PSS) buffered with LiOH to pH 7·4, or by *N*-methyl glucamine (NMG-PSS) buffered with HCl to pH 7·4. K^+-free solutions contained 145 mM NaCl, 5 mM NaH_2PO_4 and no KCl. In high-K^+ solutions, some of the NaCl was replaced by equimolar KCl. Details are given in Results and the figure legends.

$^{45}Ca^{2+}$ uptake

Synaptosomes were resuspended in Na-PSS, or Li-PSS (to deplete the internal Na^+ concentration, $[Na^+]_i$), or a mixture of the two (to obtain intermediate levels of $[Na^+]_i$). These suspensions were pre-incubated with gentle agitation for 15 min at 30 °C. Aliquots (40 μl, containing about 0·3–0·5 mg protein) were then diluted into 0·6 or 1·2 ml of either Na-PSS or NMG-PSS, or a mixture of the two. The latter solutions also contained varying amounts of $CaCl_2$ (0·02–2·0 mM), and 2–5 μCi of $^{45}Ca^{2+}$ per micromole $CaCl_2$ to initiate $^{45}Ca^{2+}$ uptake. The suspensions were incubated at 30 or 37 °C for 1–6 s (timed with a metronome); solutions for the initiation and termination (quench) of the $^{45}Ca^{2+}$ fluxes were added by manual pipetting. Details of the uptake quench, filtration and counting procedures are published (Fontana & Blaustein, 1993); one modification was that the EGTA quench solution was K^+ free for all the kinetic experiments.

For studies on the relationship between $[Na^+]_i$ and Ca^{2+} influx, synaptosomes were pre-incubated in mixtures of Ca^{2+}-free Na-PSS and Ca^{2+}-free Li-PSS (both solutions contained 25 μM EGTA and no $CaCl_2$) to vary $[Na^+]_i$. These pre-incubation solutions also contained 10 μM monensin and 1 mM ouabain, or 5 μM gramicidin D and 10 μM nigericin as well as the monensin and ouabain (see Results). In most of the figures , the $^{45}Ca^{2+}$ uptake data are expressed as 'Na^+_i-dependent $^{45}Ca^{2+}$ uptake'; in these cases, the $^{45}Ca^{2+}$ uptake by synaptosomes pre-incubated in Ca^{2+}-free Li-PSS has been subtracted from the uptake by synaptosomes pre-incubated in Ca^{2+}-free Na-PSS.

In some experiments (see Results) the synaptosomes were 'pre-depolarized' in Ca^{2+}-free 50 mM K-PSS, containing 0·2 mM EGTA and 10 μM verapamil, prior to the addition of radiotracer: 50 μl of synaptosome suspension was mixed with an equal volume of Ca^{2+}-

free 100 mM K-PSS without radiotracer. Seven seconds later, the suspension was diluted with tracer-containing solution and incubated for 1–3 s as described above.

The influence of membrane potential (V_m) on Na^+–Ca^{2+} exchanger-mediated Ca^{2+} influx was also determined: the $^{45}Ca^{2+}$ uptake from mixtures of NMG-PSS and K-PSS (all the NaCl replaced by KCl) was measured in synaptosomes pre-incubated in Na-PSS or Li-PSS. The latter was used to deplete $[Na^+]_i$ so that the Na^+_i-dependent component could be calculated. The V_m was estimated as $V_m = 60 \log([K^+]_o / [K^+]_i)$ (mV), assuming a $[K^+]_i$ of 120 mM, where $[K^+]_o$ is the external K^+ concentration and $[K^+]_i$ is the internal K^+ concentration (Blaustein & Goldring, 1975).

$^{45}Ca^{2+}$ efflux

Synaptosomes were loaded with $^{45}Ca^{2+}$ by depolarizing them for 9 s in 100 K-PSS; the Ca^{2+} load was modulated by varying the $CaCl_2$ concentration from 0·2 to 1·2 mM in the 100 mM K-PSS. Alternatively, synaptosomes were loaded with $^{45}Ca^{2+}$ by Na^+–Ca^{2+} exchange by incubating them for 9 s in NMG-PSS containing 1·2 mM $CaCl_2$. $^{45}Ca^{2+}$ uptake was halted with 3 ml of ice-cold EGTA quench solution containing (mM): 145 NMG, 3 EGTA, 5 KCl, 1·2 $MgCl_2$ and 10 Hepes adjusted to pH 7·4). The suspensions were filtered and the synaptosomes trapped on the glass fibre filters (Schleicher & Schuell No. 25) were washed 5 times with quench solution. $^{45}Ca^{2+}$ efflux was initiated immediately thereafter by exposing the synaptosomes trapped on the filters to 1 ml of either Na-PSS or NMG-PSS at 37 °C; the efflux was terminated by vacuum filtration after 1 or 2 s. Ca^{2+} was omitted from the efflux solutions to minimize tracer ($^{40}Ca^{2+}$–$^{45}Ca^{2+}$) exchange. In some instances (see Results) the efflux solutions contained 10 mM caffeine or 10 μM carbonyl cyanide *p*-trifluoromethoxyphenylhydrazone (FCCP), or both. The radioactivity of both filter and filtrate were determined by liquid scintillation methods. Appropriate 'filter blanks' and 'filtrate blanks' (obtained when synaptosomes were omitted) were subtracted from the respective gross counts.

The V_m of the synaptosomes was altered in some efflux experiments by varying the K^+ concentration in the efflux solutions: the $[Na^+]_o$ in these solutions was either 75 or 4·7 mM (Na^+ replaced by NMG), and the sum of $[Na^+]_o + [K^+]_o$ + external NMG concentration ($[NMG]_o$) was 150 mM.

Protein determinations

Synaptosome protein content was measured with the Pierce Micro BSA method (Pierce Chemical Co., Rockford, IL, USA). Incubation fluid-specific activities were measured in all experiments so that tracer fluxes could be calculated in terms of picomoles per milligram protein per second.

Statistical analysis

All measurements were made on replicate samples as described in Results. Data are presented as mean values ± S.E.M. Comparisons between means were made using Student's *t* test for unpaired data. Where indicated, the data were fitted to theoretical curves, or least-squares linear regressions were calculated with SigmaPlot 4.1 software (Jandel Scientific, Corte Madera, CA, USA).

Standard errors for the Na^+_i-dependent (ΔNa^+_i) fluxes (S.E. ΔNa^+_i) were calculated according to the equation (cf. Nachshen & Blaustein, 1979):

$$\text{S.E. } \Delta Na^+_i = \sqrt{\{[\text{S.E. } J(Na^+_i)]^2 + [\text{S.E. } J(Li^+_i)]^2\}}, \quad (1)$$

where [S.E. $J(Na^+_i)$] is the standard error of the Ca^{2+} uptake by

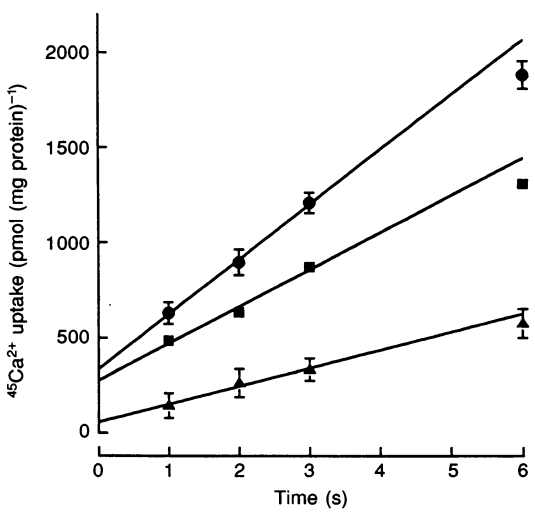

Figure 1. Time course of $^{45}Ca^{2+}$ uptake by synaptosomes incubated in Na-PSS containing 1·2 mM $CaCl_2$ labelled with tracer $^{45}Ca^{2+}$

The synaptosomes were pre-incubated for 15 min either in Na-PSS (●) or in Li-PSS (■) containing 0·2 mM $CaCl_2$. The difference between these two Ca^{2+} uptakes is the Na^+_i-dependent component (▲). The regression lines are the least-squares fits to the 1–3 s time points, only. The regression line for the Na^+_i-dependent Ca^{2+} uptake has a slope of 95 ± 14 pmol (mg protein)$^{-1}$ s^{-1}. The data are the means for 3 experiments (± S.E.M.), with four replicate determinations for each condition in each experiment. Temperature was 30 °C.

Na^+-loaded synaptosomes, and [S.E.$J(Li_i^+)$] is the standard error of the Ca^{2+} uptake by Li^+-loaded synaptosomes. Comparable formulae were used to calculate the standard errors of the 'Na_o^+-inhibitable' Ca^{2+} uptake and the Na_o^+-dependent Ca^{2+} efflux.

RESULTS

Time course of $^{45}Ca^{2+}$ uptake by synaptosomes: measurement of 'initial rates'

Figure 1 illustrates the time course of Ca^{2+} uptake by rat brain synaptosomes incubated at 30 °C in standard Na-PSS containing 1·2 mM $CaCl_2$ labelled with $^{45}Ca^{2+}$. The synaptosomes were pre-incubated in either Li-PSS (0 mM Na^+, to deplete $[Na^+]_i$; ■) or Na-PSS (145 mM Na^+; ●) containing 0·2 mM $CaCl_2$. The linearity of both curves for the first 3 s suggests that the uptakes correspond to initial rates of Ca^{2+} influx of about 290 pmol (mg protein)$^{-1}$ s^{-1} for control synaptosomes pre-incubated in Na-PSS, and 195 pmol (mg protein)$^{-1}$ s^{-1} for synaptosomes pre-incubated in Li-PSS. The apparent Ca^{2+} uptake at 'zero time' (ordinate intercept), about 300 pmol (mg protein)$^{-1}$, may correspond to the 'background' extracellular tracer retained on the filters. The difference between these two curves, the Na_i^+-dependent Ca^{2+} uptake (▲), probably corresponds to the Na^+–Ca^{2+} exchange component (see below), with a rate of about 95 ± 14 pmol (mg protein)$^{-1}$ s^{-1} under these control conditions. Thus, the Na^+–Ca^{2+} exchange may account for about one-third of the total Ca^{2+} influx in synaptosomes under 'resting' conditions.

Lowering $[Na^+]_o$ also influenced the rate of Ca^{2+} uptake: Fig. 2*A* illustrates the effects of internal and external monovalent cations on the time course of $^{45}Ca^{2+}$ uptake. The synaptosomes were pre-incubated for 15 min in either Na-PSS or Li-PSS; $^{45}Ca^{2+}$ uptake (1–6 s; 30 °C) was then determined in either NMG-PSS (4·7 mM Na^+) or Na-PSS containing 0·2 mM Ca^{2+} labelled with tracer. In all four conditions, the uptake was linear with time, which suggests that these, too, are initial rates. All four lines extrapolated to 'zero time' values of about 400–500 pmol (mg protein)$^{-1}$; this 'background' did not depend on either the internal or external monovalent cations. After subtraction of this background, the rate of $^{45}Ca^{2+}$ uptake (indicated by the slope of the line) was relatively slow when Li^+-loaded synaptosomes were studied (open symbols), or when Na^+-loaded synaptosomes were incubated in Na^+-rich media (■). The rate of $^{45}Ca^{2+}$ uptake was much greater when synaptosomes were pre-incubated in Na-PSS and then tested in NMG-PSS containing $^{45}Ca^{2+}$ (●).

The components of uptake that were affected by the changes in $[Na^+]_o$ and $[Na^+]_i$ (i.e. the difference curves) are shown in Fig. 2*B*. The Na_i^+-dependent Ca^{2+} uptake (the uptake by Na^+-loaded synaptosomes minus the uptake by Li^+-loaded synaptosomes; △) was greatly increased when $[Na^+]_o$ was reduced (▲). In other words, external Na^+ inhibited this $^{45}Ca^{2+}$ uptake. This 'Na_o^+-inhibitable' Ca^{2+} uptake into Na^+-loaded synaptosomes (▽) was nearly identical in magnitude to the Na_i^+-dependent uptake

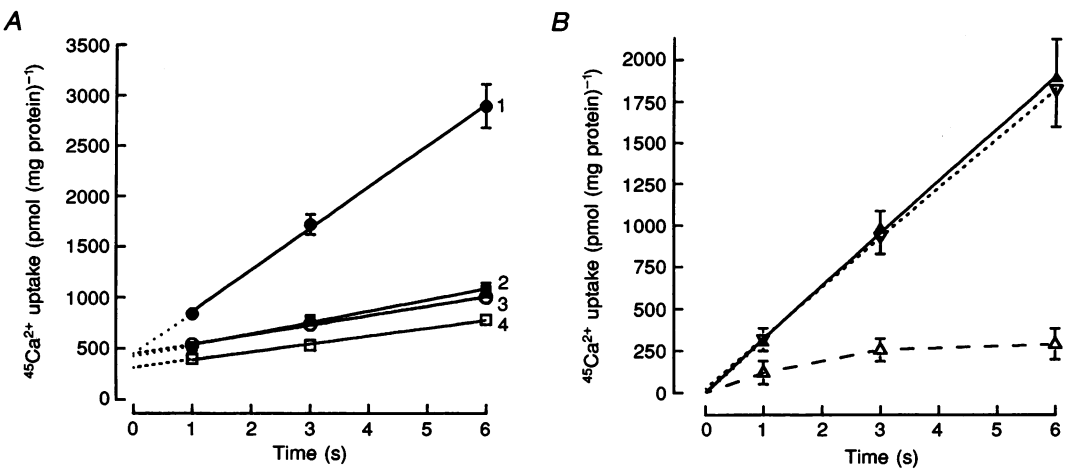

Figure 2. Effects of intra- and extracellular Na^+ on the time course of $^{45}Ca^{2+}$ uptake by synaptosomes from media containing 0·2 mM Ca^{2+}

In *A*, the synaptosomes were pre-incubated in either Na-PSS (●, ■), or in Li-PSS to deplete internal Na^+ (○, □). The synaptosomes were then diluted into either Na-PSS (145 mM Na^+; □, ■) or NMG-PSS (4·7 mM Na^+; ○, ●) containing 0·2 mM Ca^{2+} labelled with $^{45}Ca^{2+}$ for measurement of Ca^{2+} uptake at 30 °C. Each symbol represents the mean ± S.E.M. of data from 3 experiments (○, □) or 7 experiments (●, ■); in each experiment, 4 replicates were measured for each data point. *B* shows difference curves from the data in *A*. The curves illustrate the Na_i^+-dependent uptake with $[Na^+]_o$ = 145 mM (curve 2 minus curve 4 in *A*; △) and with $[Na^+]_o$ = 4·7 mM (curve 1 minus curve 3 in *A*; ▲), and the Na_o^+-inhibitable Ca^{2+} uptake (curve 1 minus curve 2 in *A*; ▽). The lines in both *A* and *B*, except for the difference curve represented by △ in *B*, are the calculated least-squares regression lines. The dashed line in *B* (△) was drawn through the data points and extrapolated to the origin.

measured in NMG-PSS (▲) because the Ca^{2+} uptake by Li^+-loaded synaptosomes incubated in NMG-PSS was comparable to the Ca^{2+} uptake by Na^+-loaded synaptosomes incubated in Na-PSS (Fig. 2*A*). Since the Na_o^+-inhibitable Ca^{2+} uptake was also dependent upon internal Na^+ (Fig. 2*B*), we will refer to both the Na_i^+-dependent and Na_o^+-inhibitable components, interchangeably, as Na^+–Ca^{2+} exchange-mediated Ca^{2+} uptake. In most subsequent experiments, however (as indicated below), the $^{45}Ca^{2+}$ uptake was determined in synaptosomes pre-incubated in Ca^{2+}-free Li-PSS as well as in Ca^{2+}-free Na-PSS, so that the Na_i^+-dependent $^{45}Ca^{2+}$ uptake (ΔNa_i^+) component could be calculated directly.

The time course of $^{45}Ca^{2+}$ uptake was also measured in NMG-PSS containing higher concentrations of Ca^{2+} (Fig. 3). Even with $[Ca^{2+}]_o$ of 1·2 mM, the Na_o^+-inhibitable Ca^{2+} uptake (650 pmol (mg protein)$^{-1}$ s^{-1}) was linear with time for at least 3 s. The implication is that these uptakes (Fig. 3*B*) approximate initial rates. Experiments of this type were therefore used to examine some of the kinetic properties of the Na^+ gradient-dependent Ca^{2+} uptake in synaptosomes. The kinetic parameters were all calculated from one-second uptake data to minimize initial rate errors.

Dependence of $^{45}Ca^{2+}$ uptake on $[Ca^{2+}]_o$: the influence of external Na^+

Activation of the Na_i^+-dependent (and Na_o^+-inhibitable) Ca^{2+} uptake (J) by $[Ca^{2+}]_o$ was measured at three different $[Na^+]_o$ at 30 °C (Fig. 4). These data demonstrate that increasing $[Na^+]_o$ decreased the apparent maximum rate of Ca^{2+} uptake ($J_{max(app)}$), but had no significant effect on the apparent affinity for Ca^{2+}. Half-maximal activation by external Ca^{2+} ($K_{Ca(o)}$), determined by SigmaPlot curve fitting to the Michaelis–Menten equation, was constant when $[Na^+]_o$ was increased 20-fold, from 4·7 mM ($K_{Ca(o)} = 0{\cdot}24$) to 96 mM ($K_{Ca(o)} = 0{\cdot}22$) (see Fig. 4 legend). The external Na^+-dependent decrease in $J_{max(app)}$ with no significant effect on $K_{Ca(o)}$ is consistent with non-competitive inhibition by Na^+. This is illustrated by the double reciprocal (Lineweaver–Burk) plot in Fig. 4*B*: the ordinate intercepts equal the $1/J_{max(app)}$ corresponding to the respective $[Na^+]_o$. The mean $K_{Ca(o)}$, determined from Michaelis–Menten equation curve fits for all three $[Na^+]_o$, was 0·23 ± 0·03 mM ($n = 11$). Then, taking the maximal J in the absence of inhibition by external Na^+ (J_{max}) to be 1530 pmol Ca^{2+} (mg protein)$^{-1}$ s^{-1}, and assuming that 2 Na^+ ions co-operatively inhibit the uptake of 1 Ca^{2+} ion (see below), the apparent mean inhibitory constant for Na_o^+ ($\bar{K}_{I(Na)}$) was calculated to be ~60 mM for $[Na^+]_o$ of 48–96 mM (Fig. 4 legend).

Inhibition of the Na_i^+-dependent Ca^{2+} uptake by external Na^+ was explored further by examining the effect of varying $[Na^+]_o$ at three different $[Ca^{2+}]_o$ (Fig. 5). These results (see, especially, the Dixon plot in Fig. 5*B*) confirm that the interaction between external Na^+ and Ca^{2+} is non-competitive. Furthermore, $\bar{K}_{I(Na)}$ was ~50 mM, and was independent of $[Ca^{2+}]_o$ for $[Ca^{2+}]_o$ between 0·1 and 1·2 mM; these $\bar{K}_{I(Na)}$ values are not very different from those obtained from the Ca^{2+} activation curves (Fig. 4). (Indeed, a slightly low $\bar{K}_{I(Na)}$ is expected because the Ca^{2+} uptake is not completely inhibited by 145 mM Na^+, the reference used for

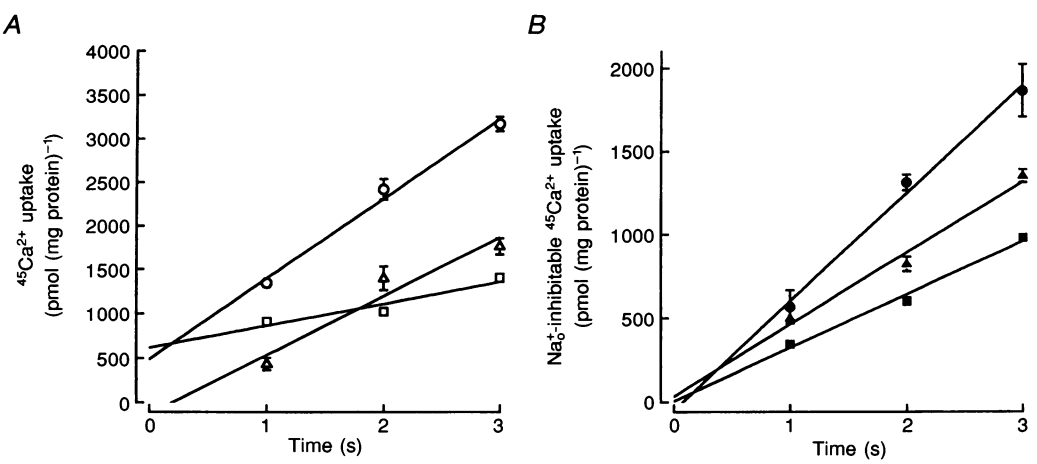

Figure 3. Na_o^+-inhibitable Ca^{2+} uptake time course curves at different $[Ca^{2+}]_o$

A, representative original data for an experiment at $[Ca^{2+}]_o = 1{\cdot}2$ mM. The linear regression lines correspond to the $^{45}Ca^{2+}$ uptake from NMG-PSS (○), the uptake from Na-PSS (□), and the difference curve (△ = uptake from NMG-PSS minus uptake from Na-PSS = 'Na_o^+-inhibitable Ca^{2+} uptake'). *B*, mean Na_o^+-inhibitable Ca^{2+} uptake ($J_{\Delta Na(o)}$) for $[Ca^{2+}]_o = 0{\cdot}2$ mM (■); 0·5 mM (▲); and 1·2 mM (●). Each symbol represents the mean ± S.E.M. of data from 4 (●) or 3 (▲ and ■) experiments; in each experiment, 4 replicates were measured for each data point. The least-squares regression lines correspond to Na_o^+-inhibitable Ca^{2+} influx rates of 318 ± 5, 429 ± 18, and 650 ± 120 pmol (mg protein)$^{-1}$ s^{-1} for $[Ca^{2+}]_o = 0{\cdot}2$, 0·5 and 1·2 mM, respectively. In all experiments, the synaptosomes were pre-incubated in Na-PSS with 0·2 mM Ca^{2+}. Temperature was 30 °C.

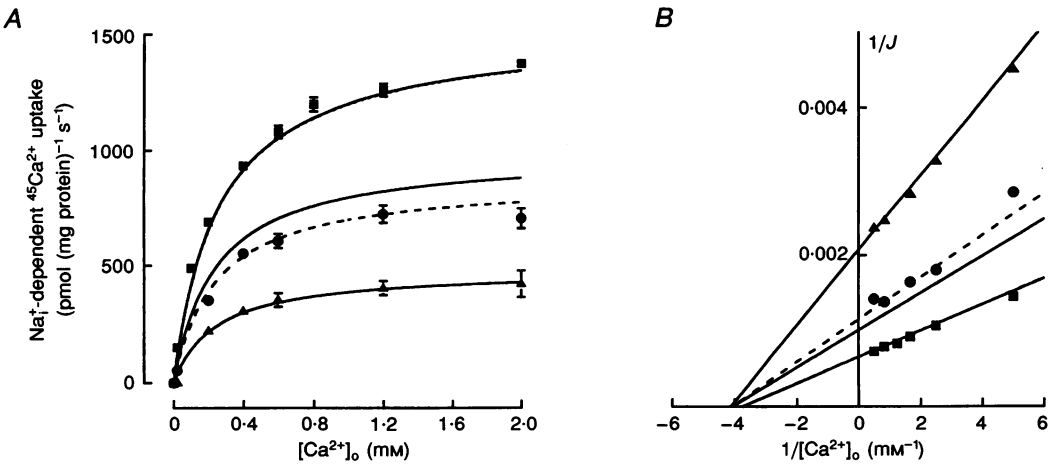

Figure 4. Activation of Na_i^+-dependent Ca^{2+} uptake by $[Ca^{2+}]_o$

Data are shown for $[Na^+]_o = 4{\cdot}7$ mM (■), 48 mM (●) and 96 mM (▲); the Na_i^+-independent Ca^{2+} uptake has been subtracted. In the low-$[Na^+]_o$ media, Na-PSS was replaced by NMG-PSS during incubation with $^{45}Ca^{2+}$. For each curve in each experiment, 4 replicates were measured for each condition (± internal Na^+); each data point corresponds to the Na_i^+-dependent Ca^{2+} uptake (J). *A* shows averaged data from 3 experiments, each with $[Na^+]_o = 48$ and 96 mM, and 5 experiments with $[Na^+]_o = 4{\cdot}7$ mM, all at 30 °C. $K_{Ca(o)}$ (the $[Ca^{2+}]_o$ at half-maximal activation) was obtained by fitting each curve in each experiment to the Michaelis–Menten equation using SigmaPlot. The mean $K_{Ca(o)}$ values are: $0{\cdot}24 \pm 0{\cdot}03$, $n = 5$ ($[Na^+]_o = 4{\cdot}7$ mM); $0{\cdot}23 \pm 0{\cdot}04$, $n = 3$ ($[Na^+]_o = 48$ mM); and $0{\cdot}22 \pm 0{\cdot}03$, $n = 3$ ($[Na^+]_o = 96$ mM). The overall mean $K_{Ca(o)} = 0{\cdot}23 \pm 0{\cdot}01$, $n = 11$. The smooth Na_i^+-dependent Ca^{2+}-influx (J) curves were calculated fits to the product of: (1) a two-substrate (Ca^{2+} and M^+) ordered bi bi activation process (cf. Segel, 1976, pp. 295–297; and see text), in which activation is proportional to:

$$A = \left(\frac{([Ca^{2+}]_o \times [M^+]_o)}{(K_{Ca(o)} \times K_M) + (K_M \times [M^+]_o) + ([Ca^{2+}]_o \times [M^+]_o)} \right); \quad \text{(L1)}$$

and (2) non-competitive inhibition by the co-operative action of two Na^+ ions (Segel, 1976, pp. 252–255; and see Fig. 5*B* and text), where inhibition is proportional to:

$$B = \left\{ 1 \Big/ 1 + \left(\frac{([Na^+]_o)^2}{(\bar{K}_{I(Na)})^2} \right) \right\}, \quad \text{(L2)}$$

where $K_{Ca(o)}$ is the calculated $[Ca^{2+}]_o$ at half-maximal activation, and $\bar{K}_{I(Na)}$ is the calculated mean $[Na^+]_o$ required for half-maximal inhibition of the Ca^{2+} influx. K_M is the alkali metal ion concentration, $[M^+]_o$, required for half-maximal activation of Ca^{2+} influx by alkali metal ions (see Figs 5 and 6, and related text). The Na_i^+-dependent Ca^{2+} uptake is then given by (see text eqn (2)):

$$J = J_{max} \times A \times B, \quad \text{(L3)}$$

where J_{max} is the calculated apparent maximal Ca^{2+} influx at saturating $[Ca^{2+}]_o$, and saturating $[M^+]_o$ (the total alkali metal ion concentration), in the absence of inhibition by Na^+. The continuous line curves in *A* were fitted to eqn (L3) with the following kinetic constants: $K_{Ca(o)} = 0{\cdot}23$ mM, $K_M = 1$ mM, $\bar{K}_{I(Na)} = 65$ mM, and $J_{max} = 1530$ pmol (mg protein)$^{-1}$ s^{-1}. The data for $[Na^+]_o = 48$ mM fit better with $\bar{K}_{I(Na)} = 55$ mM (dashed line). The data for $[Na^+]_o = 4{\cdot}7$ mM fit equally well with both values of $\bar{K}_{I(Na)}$. *B*, double reciprocal (Lineweaver–Burk) plot of the data from *A*. The calculated regression lines (text eqn (2)) intersect the abscissa at nearly the same point; they do not intersect at the ordinate intercept. This indicates that external Na^+ is a non-competitive inhibitor of Ca^{2+} influx. The abscissa intercepts ($= -1/K_{Ca(o)}$) correspond to $K_{Ca(o)} = 0{\cdot}25$, $0{\cdot}29$ and $0{\cdot}23$ mM for $[Na^+]_o = 4{\cdot}7$, 48 and 96 mM, respectively. $\bar{K}_{I(Na)}$ can be calculated from the ordinate intercept ($= 1/J_{max(app)}$) (cf. text eqn (2) with $[Ca^{2+}]_o \gg K_{Ca(o)}$ and $[M^+]_o \gg K_M$):

$$J = J_{max(app)} \left(1 + \frac{([Na^+]_o)^2}{(\bar{K}_{I(Na)})^2} \right), \quad \text{(L4)}$$

with $J_{max} = 1530$ pmol (mg protein)$^{-1}$ s^{-1}, $\bar{K}_{I(Na)} = 55$ mM (dashed line) and 65 mM (continuous line) at $[Na^+]_o = 48$ and 96 mM, respectively; the two lines were superimposable for $[Na^+]_o = 4{\cdot}7$ mM.

these calculations (see Fig. 5*B* legend).) Hill plots of the data for $[Na^+]_o$ of 10–125 mM yielded Hill coefficients of 1·9–2·0 (not shown); the implication is that two Na^+ ions act co-operatively to inhibit the uptake of one Ca^{2+}. This is consistent with the fact that the Dixon plot of $1/J$ *versus* $([Na^+]_o)^2$ produces straight lines that meet at the abscissa intercept (Fig. 5*B*). In sum, these data indicate that, with respect to the inhibition of Ca^{2+} uptake by external Na^+, external Ca^{2+} does not affect the affinity for Na^+ (Fig. 5*B*) and, conversely, external Na^+ does not affect the affinity for Ca^{2+} (Fig. 4*B*).

Activation of Na_i^+-dependent Ca^{2+} uptake by alkali metal ions

The curves in Fig. 5*A* do not exhibit monotonic inhibition by Na^+. The curves are actually biphasic: low external Na^+ concentrations (< 10 mM) activate the Ca^{2+} uptake. Indeed, this type of activation of the Na^+–Ca^{2+} exchanger by alkali metal ions, including Na^+, has previously been observed in squid axons (Baker, Blaustein, Hodgkin & Steinhardt, 1969; Blaustein, 1977; Allen & Baker, 1986) and mammalian cardiac muscle (Miura & Kimura, 1989; Gadsby, Noda, Shepherd & Nakao, 1991). Figure 6*A* shows that this activation of the Na_i^+-dependent Ca^{2+} uptake occurs with low concentrations (5–10 mM) of all alkali metal ions: Li^+, K^+, Rb^+ and Cs^+, as well as Na^+. The activation of Ca^{2+} uptake by $[Na^+]_o \leqslant 10$ mM and $[K^+]_o$ (Fig. 6*B*), and inhibition by higher $[Na^+]_o$ (Fig. 5), accounts for the biphasic nature of the J *versus* $[Na^+]_o$ curves illustrated in Fig. 5*A*.

The kinetics of activation of Ca^{2+} uptake by external Na^+ and K^+ are illustrated in Fig. 6*B*. The apparent concentrations required for half-maximal activation by these two ions ($K_{M(Na)}$ and $K_{M(K)}$, respectively) were 0·12 and 0·10 mM. These are almost certainly underestimates because of the incomplete removal of extracellular K^+ and Na^+. Furthermore, as illustrated in Fig. 5*A*, the activating effects of K^+, and low concentrations of Na^+, appear to be somewhat additive or synergistic: the Na_i^+-dependent Ca^{2+} uptake with 4·7 mM Na^+ + 5 mM K^+ (both saturating concentrations; see Fig. 6*B*) is significantly greater than with either cation alone.

The dependence of the K^+ activation of Ca^{2+} uptake on $[Ca^{2+}]_o$ is shown in Fig. 6*C* and, as a double-reciprocal plot, in Fig. 6*D*. These data are limited by the relatively high affinity for K^+ (Fig. 6*B*) and by the difficulty in precisely

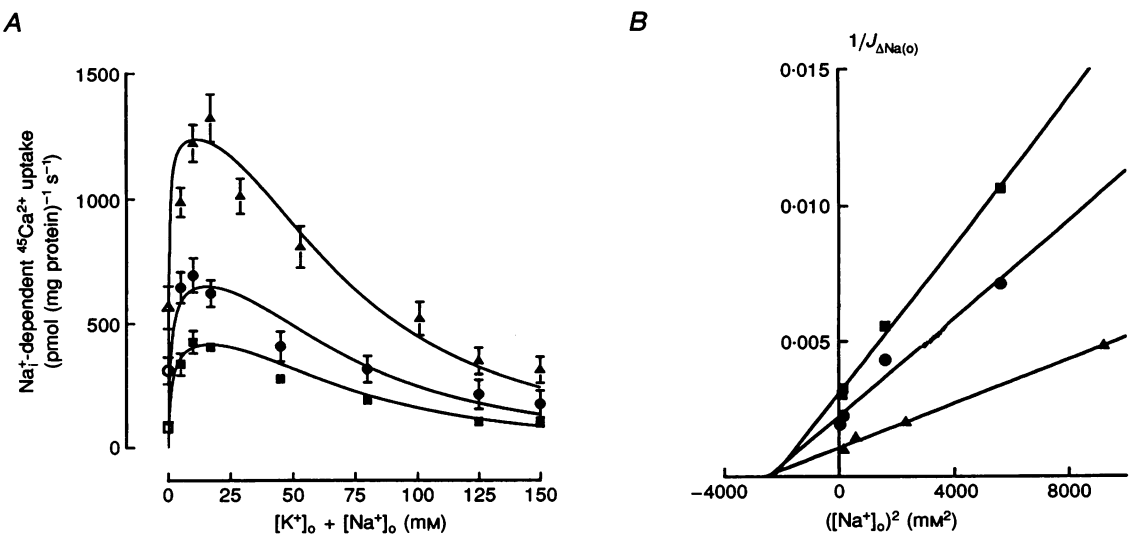

Figure 5. Activation of Na_i^+-dependent Ca^{2+} uptake by external Na^+ and K^+, and inhibition by external Na^+

Synaptosomes were pre-incubated in Na-PSS or Li-PSS; $^{45}Ca^{2+}$ uptake was then measured in mixtures of Na-PSS and NMG-PSS at 30 °C with $[Ca^{2+}]_o$ = 1·2 mM (△, ▲), 0·2 mM (○, ●), or 0·1 mM (□, ■), and the $[K^+]_o$ + $[Na^+]_o$ indicated on the abscissa (open symbols, $[K^+]_o$ = 0 mM; filled symbols, $[K^+]_o$ = 5 mM). The Na_i^+-independent Ca^{2+} uptake (in Li^+-loaded synaptosomes) has been subtracted. The symbols are the means of data from 3 to 5 experiments (4 replicates for each data point in each experiment). In *A*, the smooth curves were calculated from text eqn (2), using the following kinetic constants: $K_{Ca(o)}$ = 0·23 mM (see Fig. 4 legend), K_M = 2 mM, $\bar{K}_{I(Na)}$ = 70 mM, and J_{max} = 1530 pmol (mg protein)$^{-1}$ s^{-1}. *B* shows a Dixon plot (see Segel, 1976, p. 256) of the data in *A* for values of $[Na^+]_o \geqslant 10$ mM; the Na_i^+-dependent Ca^{2+} uptake from Na-PSS (with 145 mM Na^+) has been subtracted to obtain the Na_o^+-inhibitable flux ($J_{\Delta Na(o)}$). The abcissa units are given in terms of $([Na^+]_o)^2$; the resulting regression curves are linear, which indicates that two Na^+ ions act co-operatively to inhibit the uptake of one Ca^{2+}. The linear least-squares regression lines intersect at the abscissa (intercept = $-(\bar{K}_{I(Na)})^2$), which indicates that $\bar{K}_{I(Na)}$ is constant (mean = 50 ± 1 mM for the 3 curves), and that the interaction between external Na^+ and Ca^{2+} is non-competitive.

controlling $[K^+]_o$ (due to leak from the synaptosomes) and V_m. Nevertheless, the apparent reduction in $K_{Ca(o)}$ as well as the increase in $J_{max(app)}$ induced by increasing $[K^+]_o$ (Fig. 6*D*) raises the possibility that alkali metal ions increase the affinity of the Na^+–Ca^{2+} exchanger for external Ca^{2+}. If that is indeed the case, these kinetics may correspond to an 'ordered bi bi' reaction sequence in which the alkali metal ion is obliged to bind before Ca^{2+}, and binding is much more rapid than Ca^{2+} translocation (Segel, 1976, pp. 295–297).

Based on the aforementioned observations, the Ca^{2+} activation data (Fig. 4*A*) and the biphasic *J versus* $[Na^+]_o$

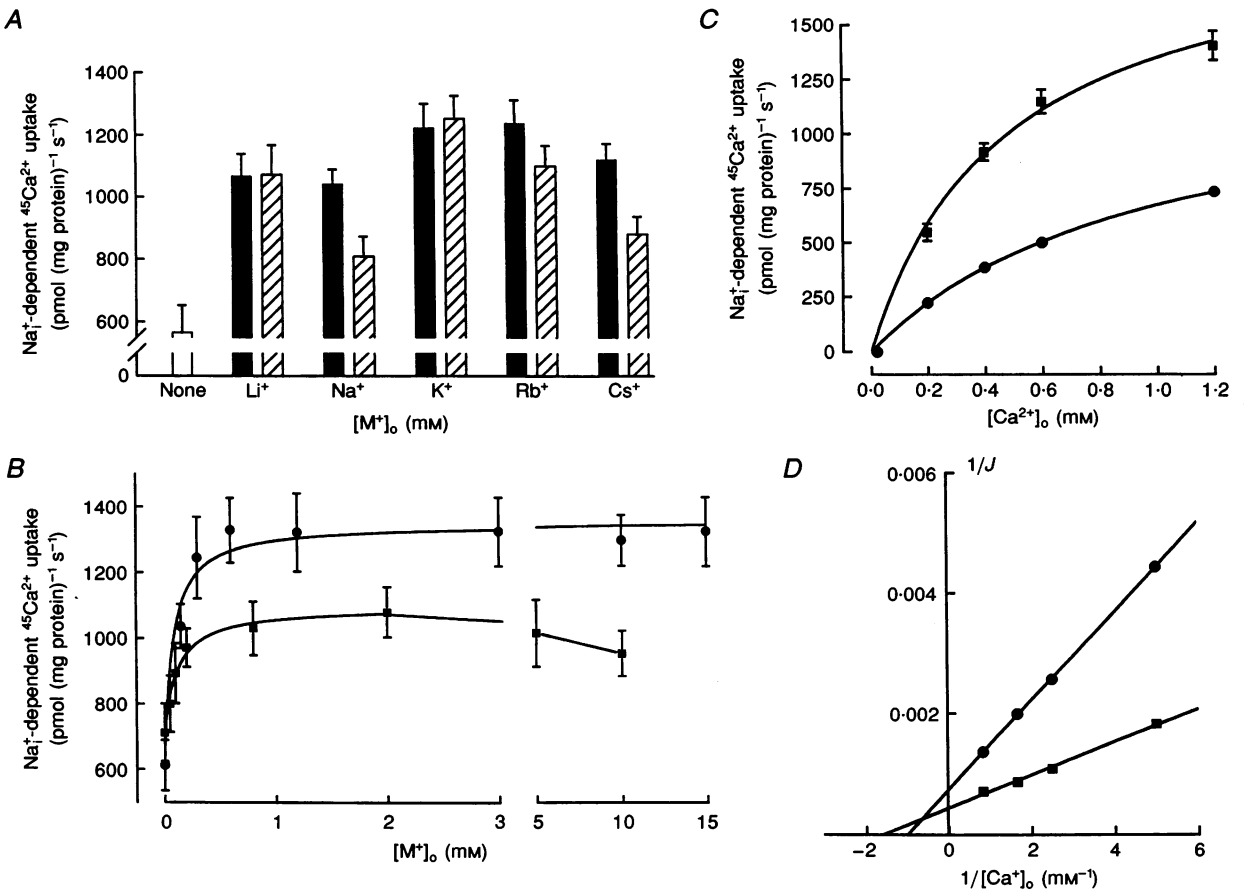

Figure 6. Activation of Na_i^+-dependent Ca^{2+} uptake by low concentrations of alkali metal ions

The nominally alkali metal ion-free medium was K^+-free NMG-PSS. All experiments were carried out at 30 °C; 4 replicate samples were obtained for each condition studied. *A* shows stimulation of Na_i^+-dependent Ca^{2+} uptake by 5 mM (■) and 10 mM (▨) concentrations of alkali metal ions in media containing 1·2 mM Ca^{2+}. The Na_i^+-independent Ca^{2+} uptake (by Li^+-loaded synaptosomes) has been subtracted. All of the alkali metal ions (5 mM) significantly increased ($P < 0·01$) the Na_i^+-dependent Ca^{2+} uptake above the nominally alkali metal ion-free control ('None'). The declines at 10 mM Na^+ and 10 mM Cs^+ were not significant ($P > 0·05$). *B* shows activation of the Na_i^+-dependent Ca^{2+} uptake by external Na^+ (■) and K^+ (●) in media containing 1·2 mM Ca^{2+}. The calculated concentrations required for half-maximal activation (based on Michaels–Menten kinetics), $K_{M(K)}$ and $K_{M(Na)}$, are 0·10 and 0·12 mM, respectively. These K_M values do not, however, take into account the alkali metal ion concentrations in the nominally alkali metal ion-free ('0 mM') media. The true K_M may therefore be much higher than indicated here; indeed, the curves in Figs 4*A* and 5*A* required values of 1–2 mM for good fits. Note the change in abscissa scale between 3 and 5 mM. *C* shows the Ca_o^{2+} dependence of the external K^+-activated, Na_i^+-dependent Ca^{2+} uptake from NMG-PSS. The Ca^{2+} uptake from nominally K^+-free media has been subtracted. Data for $[K^+]_o = 3$ (and 15) mM (■) and $[K^+]_o = 0·08$ mM (●) are shown; results for $[K^+]_o = 3$ and 15 mM were virtually identical, and have therefore been combined. *D*, double reciprocal plot of the data from *C*. The location of the intersection between the 2 regression lines suggests a mixed type of interaction: external K^+ appears to increase the affinity for Ca^{2+} (i.e. reduce $K_{Ca(o)}$) as well as increase the apparent J_{max} for Ca^{2+} uptake.

data (Fig. 5*A*) were fitted to the following equation (Fig. 4 legend, eqn (L3)):

$$J = J_{max}\left(\frac{([Ca^{2+}]_o \times [M^+]_o)}{(K_{Ca(o)} \times K_M) + (K_M \times [M^+]_o) + ([Ca^{2+}]_o \times [M^+]_o)}\right) \times \left(1 \Big/ 1 + \left\{\frac{([Na^+]_o)^2}{(K_{I(Na)})^2}\right\}\right), \quad (2)$$

where $[M^+]_o$ is the concentration of the activating external monovalent cation. This equation corresponds to the product of an ordered bi bi activation process involving alkali metal ions (M^+) and Ca^{2+} (Fig. 4 legend, eqn (L1)), and non-competitive inhibition by the co-operative action of two Na^+ (Fig. 4 legend, eqn (L2)). The fitted curves correspond reasonably well to the experimental data. The modest adjustment of the experimentally obtained kinetic parameters, $\bar{K}_{I(Na)}$ and $K_{M(Na)}$ may be due to the fact that, as noted above, the activating effects of Na^+ and K^+ appear to be somewhat additive or synergistic.

Dependence of Ca^{2+} uptake upon internal Na^+

Figure 7 shows the relationship between the $[Na^+]_o$ in the pre-incubation medium and the $^{45}Ca^{2+}$ uptake from NMG-PSS containing two different concentrations of Ca^{2+}, 0·2 and 1·2 mM. The pre-incubation media consisted of mixtures of Na-PSS and Li-PSS, with the Na^+ concentrations shown on the abscissa. In the experiment illustrated in Fig. 7*A*, the pre-incubation media also contained 10 μM monensin to increase Na^+ permeability and 1 mM ouabain to inhibit Na^+ extrusion (in an effort to equilibrate $[Na^+]_i$ with $[Na^+]_o$); the incubation media contained 1·2 mM Ca^{2+}. The curve is sigmoid ($n_H = 3{\cdot}1$), and saturates only at very high pre-incubation $[Na^+]_o$ levels. If $[Na^+]_i$ = pre-incubation $[Na^+]_o$, the apparent mean $\bar{K}_{Na(I)}$ (the $[Na^+]_i$ required for half-maximal activation of Ca^{2+} influx) seems unexpectedly high (74 mM). Thus, it might appear that very little Na^+–Ca^{2+} exchanger-mediated Ca^{2+} entry is activated by the expected normal $[Na^+]_i$ (< 10 mM). The latter observation seems to be inconsistent with the data in Figs 1 and 3, but can be explained if Na^+ and K^+ do not equilibrate across the plasma membrane under these pre-incubation conditions (i.e. the $[Na^+]_i$ values are substantially lower than the pre-incubation $[Na^+]_o$ levels) because of restricted K^+ and proton exchange.

To circumvent this problem and to equilibrate internal and external Na^+ more completely, some preparations (Fig. 7*B*) were pre-incubated in Na-PSS and Li-PSS mixtures that contained 10 μM nigericin (to increase proton permeability) and 5 μM gramicidin D (to increase K^+ permeability), as well as monensin and ouabain. Under these circumstances, with $[Ca^{2+}]_o$ of 1·2 mM, the apparent $\bar{K}_{Na(I)}$ was about 28 mM, which seems more realistic. The foot and rising phase of the $[Na^+]_i$ activation curve were then very well fitted by the Hill equation with $n_H = 3{\cdot}0$, which is consistent with the view that three internal Na^+ ions are required to activate the entry of one Ca^{2+}. The maximum rate of Ca^{2+} uptake (i.e. with a high Na^+ concentration in the pre-incubation (= intracellular) medium) was significantly reduced, however; perhaps this was due to a large decline in $[K^+]_i$, and a consequently large change in V_m.

When $[Ca^{2+}]_o$ was lowered to 0·2 mM, results very similar to those in Fig. 7*B* were obtained, although the apparent $\bar{K}_{Na(I)}$ was then only about 16 mM (Fig. 7*C*). The higher $\bar{K}_{Na(I)}$ at $[Ca^{2+}]_o$ of 1·2 mM might be an overestimate if the larger influx of Ca^{2+} under these circumstances interferes with the activation by internal Na^+. Alternatively, a decline in $\bar{K}_{Na(I)}$ with decreasing $[Ca^{2+}]_o$ might be expected if the exchange proceeds via a consecutive (sequential) mechanism in which the transport of three Na^+ ions alternates with that of one Ca^{2+} ion (Miura & Kimura, 1989; Li & Kimura, 1991; contrast Milanick, 1991).

Effect of membrane potential on Ca^{2+} uptake

To test the effect of V_m on Na^+–Ca^{2+} exchanger-mediated Ca^{2+} uptake, we determined the influence of raised $[K^+]_o$ on the Na_i^+-dependent Ca^{2+} uptake from low-Na^+ media. The data are graphed as a function of $\log[K^+]_o$ in Fig. 8 (circles); the upper abscissa indicates the calculated V_m (Blaustein & Goldring, 1975). This component of Ca^{2+} uptake increased with increasing $[K^+]_o$, as expected if depolarization promotes the exit of net positive charge associated with an exchange of three or more Na^+ ions for one entering Ca^{2+}.

An Eyring rate theory model was used to estimate the voltage dependence of the voltage-sensitive step (Läuger, 1991*a*, *b*; Niggli & Lederer, 1993). Accordingly, the data were fitted to the equation:

$$J = J_o \exp\left(\frac{zFV_m}{2RT}\right), \quad (3)$$

where J is the Na_i^+-dependent Ca^{2+} influx (which corresponds to the net outward current) at any V_m (mV), and J_0 is the Ca^{2+} influx at $V_m = 0$ mV. R, T and F have their usual meanings, and z is the fraction of the membrane electric field through which an elementary positive charge moves during the rate-limiting step during each complete Ca^{2+} influx (and Na^+ efflux) cycle. The fitted line corresponds to one elementary positive charge moving out of the terminals through about 58% of the membrane field (or, alternatively, +0·58 elementary charges moving through 100% of the electric field). The implication is that this is not the only voltage-sensitive step in the cycle because the net total outward charge movement is +1·0 through the entire electric field if the coupling ratio is 3 Na^+ : 1 Ca^{2+} (see Discussion).

'Initial rates' of Na_o^+-dependent Ca^{2+} efflux from synaptosomes

To determine whether the maximum rate of exchanger-mediated Ca^{2+} efflux was comparable to that of Ca^{2+} influx, 'initial rates' of Na_o^+-dependent Ca^{2+} efflux were measured after loading the synaptosomes with $^{45}Ca^{2+}$. Figure 9*A* shows the $^{45}Ca^{2+}$ content (calibrated for specific activity) of synaptosomes immediately after loading the terminals with tracer via Na^+–Ca^{2+} exchange (i.e. by reducing $[Na^+]_o$ in the loading solution): this is the 'zero time' point on the

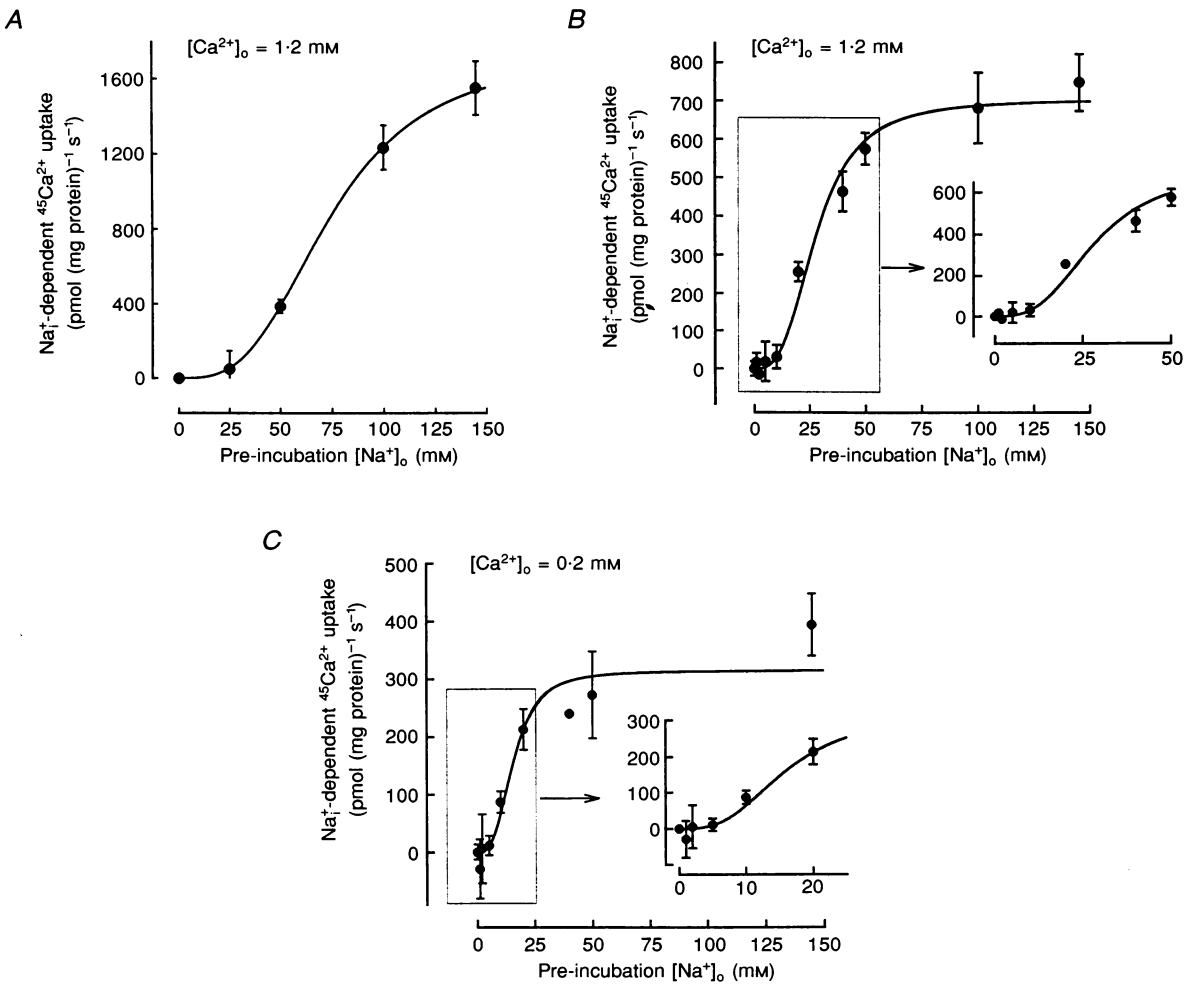

Figure 7. Dependence of Ca^{2+} uptake on $[Na^+]_i$

Synaptosomes were pre-incubated for 15 min in mixtures of Na-PSS and Li-PSS containing the $[Na^+]_o$ shown on the abscissa. The pre-incubation media also contained 10 μM monensin and 1 mM ouabain (*A*) or 10 μM monensin, 1 mM ouabain, 5 μM gramicidin D and 10 μM nigericin (*B* and *C*). $^{45}Ca^{2+}$ uptake was then measured in either Na-PSS or NMG-PSS containing 1·2 mM Ca^{2+} (*A* and *B*) or 0·2 mM Ca^{2+} (*C*) at 30 °C. The symbols indicate the differences (i.e. the Na_o^+-inhibitable = Na_i^+-dependent Ca^{2+} uptake). Data from 2 representative experiments are shown; 4 replicates were obtained for each condition in each experiment; error bars indicate ± S.E.M. The Ca^{2+} uptake (J) curves were fitted to the Hill equation (Segel, 1976, p. 309):

$$J = J_{max(app)}\left(\frac{([Na^+]_i)^{n_H}}{([Na^+]_i + \bar{K}_{Na(i)})^{n_H}}\right), \quad \text{(L5)}$$

where n_H is the Hill coefficient and $\bar{K}_{Na(i)}$ is the apparent $[Na^+]_i$ required for half-maximal activation of the Ca^{2+} influx. The calculated parameters for the fitted curves are:

Curve	$[Ca^{2+}]_o$	n_H	$\bar{K}_{Na(i)}$	$J_{max(app)}$
A	1·2	3·1	74	1721
B	1·2	3·0	28	702
C	0·2	3·0	16	314

where $[Ca^{2+}]_o$ and $\bar{K}_{Na(i)}$ are in mM and $J_{max(app)}$ is in pmol (mg protein)$^{-1}$ s^{-1}.

graph. The graph also shows the amount of Ca^{2+} (as $^{45}Ca^{2+}$) remaining in the synaptosomes following 1 s and 2 s exposures to Ca^{2+}-free (and tracer-free) Na-PSS or NMG-PSS without or with 10 μM FCCP. Figure 9*B* shows comparable data from a representative experiment in which the synaptosomes were loaded with $^{45}Ca^{2+}$ via voltage-gated Ca^{2+} channels (i.e. by temporarily raising $[K^+]_o$ and depolarizing the terminals). The average total Ca^{2+} load in these eight experiments was ~7200 pmol Ca^{2+} (as $^{45}Ca^{2+}$) (mg protein)$^{-1}$ (Table 1 legend). In some instances, during the 1–2 s efflux period, free cytosolic Ca^{2+} concentration ($[Ca^{2+}]_{cyt}$) was increased with either 10 μM FCCP (which uncouples oxidative phosphorylation and releases Ca^{2+} from mitochondria) or 10 mM caffeine (which releases Ca^{2+} from the endoplasmic reticulum), or both FCCP and caffeine. This presumably saturated the Ca^{2+} transport sites at the cytoplasmic face of the plasmalemma in an effort to obtain J_{max} values for the Ca^{2+} efflux.

The Na_o^+-dependent and Na_o^+-independent effluxes are summarized in Table 1. Both FCCP (Sanchez-Armass & Blaustein, 1987) and caffeine independently increased the Ca^{2+} efflux (especially the Na_o^+-dependent component). The two agents together had only a slight (non-significant) additional effect, implying that the transport systems were then saturated with Ca^{2+}. These data indicate that the J_{max} for the Na^+–Ca^{2+} exchanger-mediated Ca^{2+} efflux (i.e. the Na_o^+-dependent efflux component) is about 1800–2000 pmol (mg protein)$^{-1}$ s^{-1} (assuming a linear rate of efflux during the first 1 s), and is much larger than the Na_o^+-independent component which may correspond primarily to the plasmalemmal ATP-driven Ca^{2+} pump and Ca^{2+} 'leak'.

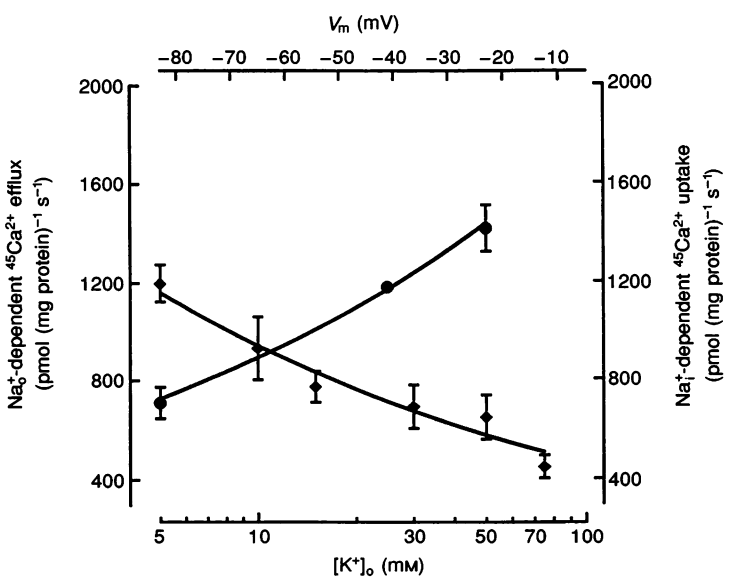

Figure 8. Effect of $[K^+]_o$ and membrane potential on Na_i^+-dependent Ca^{2+} uptake and Na_o^+-dependent Ca^{2+} efflux

For the study of Ca^{2+} uptake (●), synaptosomes were loaded with Na^+ or Li^+ by incubation for 15 min at 37 °C in Na-PSS or Li-PSS, respectively. They were then pre-depolarized by diluting 50 μl of synaptosome suspension with 50 μl Ca^{2+}- and Na^+-free (NMG) medium containing 100 mM K^+, 10 μM verapamil and 0·2 mM EGTA. Seven seconds later, $^{45}Ca^{2+}$ uptake was measured by adding 1·4 ml mixtures of NMG-PSS and K-PSS containing 0·2 mM tracer-labelled Ca^{2+} with the final $[K^+]_o$ indicated on the lower abscissa (log scale). The ordinate (right-hand scale) shows the Na_i^+-dependent Ca^{2+} uptake (uptake in synaptosomes pre-incubated in Na-PSS minus uptake in synaptosomes incubated in Li-PSS). The upper abscissa scale shows the calculated membrane potential, V_m (see Methods). The symbols are the means of data from 4 experiments, with 4 replicate determinations for each condition in each experiment. The continuous line has a slope equivalent to about a 2-fold increase in Na_i^+-dependent Ca^{2+} uptake per 60 mV depolarization. The temperature was 37 °C. For the study of Ca^{2+} efflux (◆), synaptosomes were loaded with $^{45}Ca^{2+}$ via voltage-gated Ca^{2+} channels by depolarizing the terminals for 9 s in 100 mM K-PSS containing 0·2 mM Ca^{2+}. After washing out the extracellular $^{45}Ca^{2+}$, tracer efflux was measured for 1 s at 37 °C in mixtures of Na-PSS, NMG-PSS and K-PSS. For each $[K^+]_o$, Ca^{2+} efflux was measured in media with $[Na^+]_o$ = 75 mM and $[Na^+]_o$ = 5 mM; the difference between these two fluxes, the Na_o^+-dependent Ca^{2+} efflux (◆), is plotted on the ordinate (left-hand scale). The symbols for the efflux experiments correspond to the means of data from 4 experiments, with 5 replicate determinations for each condition in each experiment. The continuous lines for both the Ca^{2+} influx and efflux curves were calculated to fit the Eyring rate theory equation (see text for details).

Table 1. Effects of external Na^+, FCCP and caffeine on $^{45}Ca^{2+}$ efflux from rat forebrain synaptosomes

Conditions	Na_o^+-dependent $^{45}Ca^{2+}$ efflux (pmol (mg protein)$^{-1}$ s^{-1})	Na_o^+-independent $^{45}Ca^{2+}$ efflux (pmol (mg protein)$^{-1}$ s^{-1})
Controls	1320 ± 80 (8)	639 ± 86 (8)
Caffeine (10 mM)	1829 ± 170 (6)**	564 ± 65 (6)
FCCP (10 μM)	1870 ± 139 (8)**	957 ± 42 (6)*
Caffeine (10 mM) + FCCP (10 μM)	2003 ± 191 (4)**	852 ± 75 (4)*

Data are the means ± S.E.M. of 1 s effluxes at 37 °C. The number of experiments (i.e. the number of synaptosome preparations) is indicated in parentheses; in each experiment, 5 replicate determinations were made for each condition. The average Ca^{2+} load (as $^{45}Ca^{2+}$) was 7197 ± 234 pmol Ca^{2+} (mg protein)$^{-1}$, $n = 8$. * $P < 0.05$ *vs.* controls; ** $P < 0.01$ *vs.* controls.

Effect of membrane potential on Na_o^+-dependent Ca^{2+} efflux

The voltage sensitivity of the Na^+–Ca^{2+} exchanger operating in the Ca^{2+} efflux mode was determined by examining the effect of varying $[K^+]_o$ at constant $[Na^+]_o$ on the Na_o^+-dependent component of Ca^{2+} efflux. The results, shown in Fig. 8 (◆), indicate that the Na_o^+-dependent Ca^{2+} efflux decreased with increasing $[K^+]_o$. These data were fitted to the same Eyring model as the one used to examine the voltage sensitivity of Ca^{2+} influx (eqn (3), above). As illustrated by the fitted line, Ca^{2+} efflux is consistent with the entry of one positive elementary charge, moving through 57% of the membrane electric field at the rate-limiting step. In the range of voltages shown here, Ca^{2+} efflux *decreased* about 2-fold with a 60 mV depolarization, whilst Ca^{2+} influx *increased* about 2-fold, with a 60 mV depolarization. Thus, the voltage-sensitive step in Ca^{2+} translocation appears to be reversible and symmetric. This is not surprising for a transport system that is directly powered by ion electrochemical gradients rather than by ATP.

DISCUSSION

The Na_i^+-dependent Ca^{2+} influx and Na_o^+-dependent Ca^{2+} efflux in rat brain synaptosomes were used as functional measures of Na^+–Ca^{2+} exchange activity. The Ca^{2+} uptake activated by lowering $[Na^+]_o$ was Na_i^+ dependent, and was also utilized to identify the Na^+–Ca^{2+} exchanger-mediated component of Ca^{2+} influx (Fig. 2*B*). Based on these definitions of the Na^+–Ca^{2+} exchanger, we employed 1 s $^{45}Ca^{2+}$ fluxes to approximate initial rates for kinetic analysis (Fig. 3). Most experiments were performed at 30 °C, rather than at 37 °C, to slow the kinetics so that some parameters could be better resolved; the lower temperature also improved synaptosome stability.

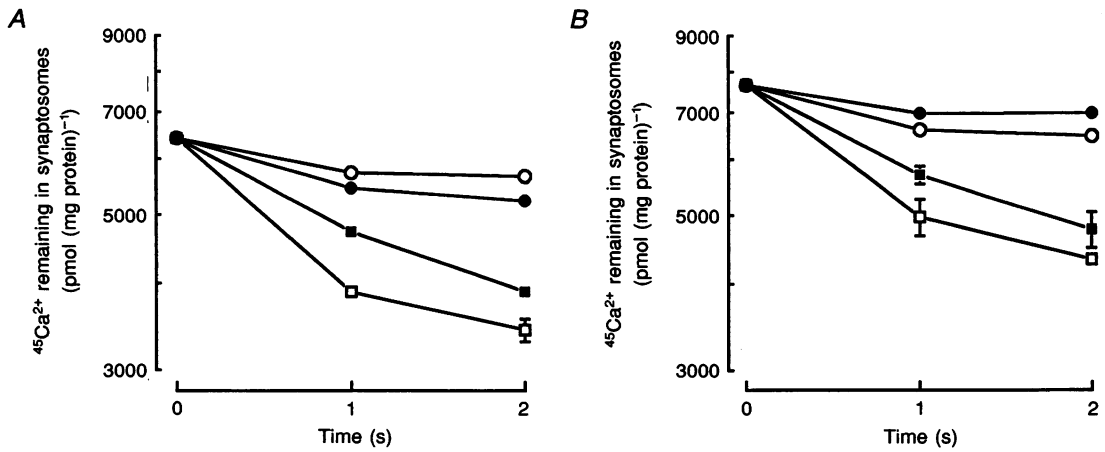

Figure 9. Effect of external Na^+ on the time course of Ca^{2+} efflux from synaptosomes

A, synaptosomes were loaded with $^{45}Ca^{2+}$ via Na^+–Ca^{2+} exchange by incubating the Na^+-loaded terminals for 9 s in NMG-PSS containing 1·2 mM Ca^{2+}. *B*, synaptosomes were loaded with $^{45}Ca^{2+}$ via voltage-gated Ca^{2+} channels (Nachshen & Blaustein, 1980) by depolarizing the terminals for 9 s in 100 mM K-PSS containing 1·2 mM Ca^{2+}. In both *A* and *B*, after washing out the extracellular $^{45}Ca^{2+}$, tracer efflux was measured for 1 and 2 s in either NMG-PSS ($[Na^+]_o = 0$ mM; circles) or Na-PSS (squares), either without (filled symbols) or with (open symbols) 10 μM FCCP (to release Ca^{2+} from overloaded mitochondria). The ordinate (log scale) shows the amount of Ca^{2+} (as tracer) remaining in the synaptosomes after 0, 1 and 2 s of efflux at 37 °C. Symbols indicate the means ± S.E.M. of 5 replicate determinations.

Kinetics: the large capacity (maximum velocity) of the Na^+–Ca^{2+} exchanger

One of the key observations is the large maximum rate of Ca^{2+} transport mediated by the Na^+–Ca^{2+} exchanger in rat brain synaptosomes. Ca^{2+} uptake data indicate that a lower-limit estimate for J_{max} (i.e. the maximal capacity) of the exchanger in the Ca^{2+} influx mode at 30 °C is about 1500 pmol (mg protein)$^{-1}$ s^{-1}. This may be compared to the J_{max} of the exchanger in the Ca^{2+} efflux mode, 1800–2000 pmol (mg protein)$^{-1}$ s^{-1} at 37 °C. The implication is that the exchanger can move Ca^{2+} into and out of the nerve terminals at similar maximal rates at the normal resting V_m. These J_{max} values correspond to a Na^+–Ca^{2+} exchanger-mediated flux of 425–575 μmol Ca^{2+} (l cell water)$^{-1}$ s^{-1} since intra-synaptosome volume is about 3·5 μl (mg protein)$^{-1}$ (Blaustein, 1975). This large Ca^{2+} flux is equivalent to a turnover of about one quarter of the total synaptosome Ca^{2+} (about 2 mmol (l cell water)$^{-1}$; Schweitzer & Blaustein, 1980) in 1 s.

The Ca^{2+} transport in normal 'resting' (non-depolarized) synaptosomes proceeds at a very much slower rate (Fig. 1). The resting Ca^{2+} influx is about 300 pmol (mg protein)$^{-1}$ s^{-1}, and about one-third of this may be Na^+–Ca^{2+} exchanger-mediated. Thus, under resting conditions, the exchanger turns over at only about 5% of its maximal rate.

Kinetics and mechanism: interactions between Na^+ and Ca^{2+}

The interference with Ca^{2+} uptake by Na^+ at the external face of the plasmalemma (Figs 4 and 5) appears to be non-competitive in synaptosomes because raising $[Na^+]_o$ reduces $J_{max(app)}$ but does not affect $K_{Ca(o)}$. The reciprocal relationship is also observed: lowering $[Ca^{2+}]_o$ does not affect $\bar{K}_{I(Na)}$, but does reduce $J_{max(app)}$. This implies that the Na^+ and Ca^{2+} do not bind to identical sites on the exchanger. These observations and conclusions differ from those in cardiac muscle reported by Reeves & Sutko (1983), and Miura & Kimura (1989), who suggested that external Na^+ is a competitive inhibitor of Ca^{2+} at the exchanger's external Ca^{2+}-binding site. In accordance with their conclusions, we observed that this interaction between external Na^+ and Ca^{2+} apparently involves 2 Na^+ ions and 1 Ca^{2+} ion. Nonetheless, it is difficult to imagine how 2 Na^+ ions (each with an ionic radius ~1) could bind to the identical site to which 1 Ca^{2+} (ionic radius ~1) binds. Thus, at least superficially, a non-competitive interaction seems more plausible. We cannot exclude the possibility that the brain and cardiac exchangers have significantly different kinetics. However, Matsuoka & Hilgemann (1992) reported that internal Na^+ and Ca^{2+} exhibit a mixed (competitive/non-competitive) interaction at the ion-binding sites that face the cytoplasm on the cardiac muscle Na^+–Ca^{2+} exchanger. Moreover, data from squid axons (Blaustein & Russell, 1975; Blaustein, 1977) are also compatible with a non-competitive or mixed-type interaction between Na^+ and Ca^{2+} at the inner surface of the plasmalemma.

Kinetics and mechanism: activation of Ca^{2+} influx by alkali metal ions

The Na^+–Ca^{2+} exchanger in rod outer segments has an absolute requirement for K^+ on the side of the membrane from which Ca^{2+} is being transported; thus, the coupling ratio is 4 Na^+ : (1 Ca^{2+} + 1 K^+) (Cervetto, Lagnado, Perry, Robinson & McNaughton, 1989). In contrast, the exchanger from mammalian heart does not require K^+ and has a coupling ratio of 3 Na^+ : 1 Ca^{2+} (Yasui & Kimura, 1990). The situation in mammalian brain has been less clear. The brain exchanger is structurally similar to the heart exchanger (Yip *et al.* 1992; Furman *et al.* 1993; Marlier *et al.* 1993). Moreover, unlike the non-homologous mammalian photoreceptor exchanger, the brain exchanger does not have an absolute requirement for K^+, although low concentrations of external K^+ apparently activate exchanger-mediated Ca^{2+} influx (Dahan, Spanier & Rahamimoff, 1991). Our findings may help to resolve this dilemma. We observed that a low concentration (1–10 mM) of any alkali metal ion (including Na^+ as well as K^+) can activate the Na_i^+-dependent Ca^{2+} influx. This is consistent with early observations on the Na^+–Ca^{2+} exchanger in squid axons (Baker *et al.* 1969) as well as with more recent work on the cardiac exchanger (Miura & Kimura, 1989; Gadsby *et al.* 1991). Thus, the activation of Na_i^+-dependent Ca^{2+} influx by low concentrations (< 2 mM) of K^+, observed by Dahan *et al.* (1991), can probably be explained by an action at the alkali metal ion activation site. This activation appears to be different from the obligatory, stoichiometric requirement for K^+ that is co-transported with Ca^{2+} on the rod photoreceptor Na^+–Ca^{2+} exchanger. The activating ion in the brain–heart exchanger does not appear to be transported because Na^+ can serve as an activating cation (Fig. 5), even though the stoichiometry of the exchange appears to be 3 Na^+ : 1 Ca^{2+} (i.e. there is no evidence that Na^+ entry is required to promote Ca^{2+} entry and Na^+ exit).

Coupling ratio and voltage sensitivity of the Na^+–Ca^{2+} exchanger in nerve terminals

Several observations support the view that the Na^+ : Ca^{2+} coupling ratio in rat brain synaptosomes is about 3 Na^+ : 1 Ca^{2+}. One is that the dependence of Ca^{2+} efflux on external Na^+ is sigmoid, with a Hill coefficient of 2·5 (Sanchez-Armass & Blaustein, 1987). In the present study, we observed that the Hill coefficient for activation of Ca^{2+} influx by internal Na^+ is about 3·0 (Fig. 7). Taken together, these data suggest that Ca^{2+} transport is dependent upon the co-operative action of 3 Na^+ ions on the opposite side of the membrane. Furthermore, the rat brain synaptic membrane exchanger is immunologically and structurally similar to the dog cardiac exchanger (Yip *et al.* 1992; Furman *et al.* 1993) which has a coupling ratio (or stoichiometry) of 3 Na^+ : 1 Ca^{2+} (Yasui & Kimura, 1990).

An exchanger with this coupling ratio should be voltage sensitive if one or more of the intermediate steps in the transport cycle is voltage sensitive (Läuger, 1991*a*, *b*).

Indeed, the nerve terminal Na^+–Ca^{2+} exchanger exhibits substantial voltage sensitivity: approximately a 2-fold change in flux per 60 mV change in membrane potential. Moreover, the voltage sensitivity is the same for both Ca^{2+} influx and efflux (Fig. 8). This voltage sensitivity is comparable to that of the exchanger in cardiac myocytes, where an e-fold change in Ca^{2+} flux per 77 mV change in voltage is observed (Crespo *et al.* 1990).

Perhaps even more interesting is the fact that the voltage-sensitive step in ion translocation appears to be symmetrical and thus reversible, as in the heart exchanger (Niggli & Lederer, 1993). The fact that this voltage sensitivity corresponds to the movement of one elementary charge through only about 58% of the membrane electric field during this step implies that there is another voltage-sensitive step in the transport cycle, since there must be a net transport of one charge through the entire field per cycle. This other voltage-sensitive step might be an ion-binding step (Gadsby, Rakowski & DeWeer, 1993; G. Fontana, R. S. Rogowski & M. P. Blaustein, unpublished data).

Physiological role(s) of the Na^+–Ca^{2+} exchanger in nerve terminals

The large capacity (J_{max}) of the nerve terminal Na^+–Ca^{2+} exchanger, and its apparent prevalence (Luther *et al.* 1992), imply that the exchanger plays an important role in nerve terminal physiology. The Na^+–Ca^{2+} exchanger has a relatively low affinity for cytoplasmic Ca^{2+} ($K_{Ca(i)}$ in the order of 10^{-6} M (Rasgado-Flores *et al.* 1989) in contrast to the plasmalemmal ATP-driven Ca^{2+} pump with a $K_{Ca(i)}$ for Ca^{2+} in the order of 10^{-7} M (DiPolo & Beaugé, 1979)). Thus, the turnover of the exchanger may be relatively slow under 'resting' (unstimulated) conditions when $[Ca^{2+}]_i$ is about 10^{-7} M (Blaustein *et al.* 1991). Nevertheless, the exchanger may modulate the resting $[Ca^{2+}]_i$, even though this level may be controlled primarily by the ATP-driven Ca^{2+} pump. More importantly, even small changes in $[Ca^{2+}]_i$ modulate the amount of Ca^{2+} in the intracellular stores in the endoplasmic reticulum (Blaustein *et al.* 1991) because more than 99·9% of the intracellular Ca^{2+} is sequestered (buffered; Duarte, Carvalho, Ferreira & Carvalho, 1991; Fontana & Blaustein, 1993). In this way, the exchanger may influence the numerous processes that are dependent upon release of Ca^{2+} from the intracellular stores (Nahorski, 1988).

The exchanger may also mediate net Ca^{2+} influx during nerve terminal depolarization. The depolarization (see Fig. 8) and increase in driving force, as well as the transient rise in $[Ca^{2+}]_i$ that activates Ca^{2+} influx mode exchange (DiPolo & Beaugé, 1987; Rasgado-Flores *et al.* 1989), should enhance exchanger-mediated Ca^{2+} entry. We have no direct information about the relative contributions of this mechanism and of Ca^{2+} entry via voltage-gated Ca^{2+} channels to the ensuing Ca^{2+} transients. Operating at maximal rate, however, the exchanger could, at most, contribute about 1–2 pmol Ca^{2+} to the total influx of about 6 pmol mg^{-1} ms^{-1} (Nachshen, 1985).

When the membrane repolarizes during the falling phase of the action potential, the driving force will favour Ca^{2+} extrusion via the exchanger. Ca^{2+} transport sites at the cytoplasmic face of the membrane will then be saturated because of the high $[Ca^{2+}]_i$ (perhaps $\sim 10^{-4}$ M (Smith & Augustine, 1988)). This will favour rapid Ca^{2+} extrusion via the exchanger. Thus, the exchanger may even help to terminate evoked transmitter release following cell activation. Most of the Ca^{2+} that enters during depolarization will, however, diffuse away from the plasmalemma, and will be rapidly buffered and sequestered. This Ca^{2+} will then be extruded from the terminals over the next 1–2 s (Blaustein, 1988). The fact that most of this Ca^{2+} efflux is Na_o^+ dependent (Fig. 9; and see Sanchez-Armass & Blaustein, 1987) suggests that the Na^+–Ca^{2+} exchanger plays a dominant role in Ca^{2+} extrusion following nerve terminal activation.

Allen, T. J. A. & Baker, P. F. (1986). Comparison of the effects of potassium and membrane potential on the calcium-dependent sodium efflux in squid axons. *Journal of Physiology* **378**, 53–76.

Andressen, C., Blümcke, I. & Celio, M. R. (1993). Calcium-binding proteins: selective markers of nerve cells. *Cell Tissue Research* **271**, 181–208.

Baker, P. F., Blaustein, M. P., Hodgkin, A. L. & Steinhardt, R. A. (1969). The influence of calcium on sodium efflux in squid axons. *Journal of Physiology* **200**, 431–458.

Blaustein, M. P. (1975). Effects of potassium, veratridine and scorpion venom on calcium accumulation and transmitter release by nerve terminals *in vitro*. *Journal of Physiology* **247**, 617–655.

Blaustein, M. P. (1977). Effects of internal and external cations and of ATP on sodium–calcium and calcium–calcium exchange in squid axons. *Biophysical Journal* **20**, 79–111.

Blaustein, M. P. (1988). Calcium transport and buffering in neurons. *Trends in Neurosciences* **11**, 438–443.

Blaustein, M. P., Goldman, W. F., Fontana, G., Krueger, B. K., Santiago, E. M., Steele, T. D., Weiss, D. N. & Yarowsky, P. J. (1991). Physiological roles of the sodium–calcium exchanger in nerve and muscle. *Annals of the New York Academy of Sciences* **639**, 254–274.

Blaustein, M. P. & Goldring, J. M. (1975). Membrane potentials in pinched-off presynaptic nerve terminals monitored with a fluorescent probe: evidence that synaptosomes have potassium diffusion potentials. *Journal of Physiology* **247**, 589–615.

Blaustein, M. P., Ratzlaff, R. W., Kendrick, N. C. & Schweitzer, E. S. (1978). Calcium buffering in presynaptic nerve terminals. I. Evidence for involvement of a nonmitochondrial ATP-dependent sequestration mechanism. *Journal of General Physiology* **72**, 15–41.

BLAUSTEIN, M. P. & RUSSELL, J. M. (1975). Sodium–calcium exchange and calcium–calcium exchange in internally dialyzed squid giant axons. *Journal of Membrane Biology* **22**, 285–312.

CERVETTO, L., LAGNADO, L., PERRY, R. J., ROBINSON, D. W. & MCNAUGHTON, P. A. (1989). Extrusion of calcium from rod outer segments is driven by both sodium and potassium gradients. *Nature* **337**, 740–743.

CRESPO, L. M., GRANTHAM, C. J. & CANNELL, M. B. (1990). Kinetics, stoichiometry and role of the Na–Ca exchange mechanism in isolated cardiac myocytes. *Nature* **345**, 618–621.

DAHAN, D., SPANIER, R. & RAHAMIMOFF, H. (1991). The modulation of rat brain Na^+–Ca^{2+} exchange by K^+. *Journal of Biological Chemistry* **266**, 2067–2075.

DIPOLO, R. & BEAUGÉ, L. (1979). Physiological role of ATP-driven calcium pump in squid axons. *Nature* **278**, 271–273.

DIPOLO, R. & BEAUGÉ, L. (1987). Characterization of the reverse Na/Ca exchange in squid axons and its modulation by Ca_i and ATP. Ca_o-dependent Na_i/Ca_o and Na_i/Na_o exchange modes. *Journal of General Physiology* **90**, 505–525.

DUARTE, C. B., CARVALHO, C. A. M., FERREIRA, I. L. & CARVALHO, A. P. (1991). Synaptosomal $[Ca^{2+}]_i$ as influenced by Na^+/Ca^{2+} exchange and K^+ depolarization. *Cell Calcium* **12**, 623–633.

FONTANA, G. & BLAUSTEIN, M. P. (1993). Calcium buffering and free Ca^{2+} in rat brain synaptosomes? *Journal of Neurochemistry* **60**, 843–850.

FURMAN, I., COOK, O., KASIR, J. & RAHAMIMOFF, H. (1993). Cloning of two isoforms of the rat brain Na^+–Ca^{2+} exchanger gene and their functional expression in HeLa cells. *FEBS Letters* **319**, 105–109.

GADSBY, D. C., NODA, M., SHEPHERD, R. N. & NAKAO, M. (1991). Influence of external monovalent cations on Na–Ca exchange current–voltage relationships in cardiac myocytes. *Annals of the New York Academy of Sciences* **639**, 140–146.

GADSBY, D. C., RAKOWSKI, R. F. & DEWEER, P. (1993). Extracellular access to the Na, K pump: pathway similar to ion channel. *Science* **260**, 100–103.

GILL, D. L., GROLLMAN, E. F. & KOHN, L. D. (1981). Calcium transport mechanisms in membrane vesicles from guinea pig brain synaptosomes. *Journal of Biological Chemistry* **256**, 184–192.

KATZ, B. (1969). *The Release of Neural Transmitter Substances.* Thomas, Springfield, IL, USA.

KHANANSHVILI, D. (1990). Distinction between the two basic mechanisms of cation transport in the cardiac Na^+–Ca^{2+} exchange system. *Biochemistry* **29**, 2437–2442.

LÄUGER, P. (1991*a*). *Electrogenic Ion Pumps.* Sinauer Associates, Sunderland, MA, USA.

LÄUGER, P. (1991*b*). Kinetic basis of voltage dependence of the Na, K-pump. In *The Sodium Pump: Structure, Mechanism, and Regulation*, ed. KAPLAN, J. H. & DE WEER, P., pp. 303–315. Rockefeller University Press, New York.

LI, J. & KIMURA, J. (1999). Translocation mechanism of cardiac Na–Ca exchange. *Annals of the New York Academy of Sciences* **639**, 48–60.

LUTHER, P. W., YIP, R. K., BLOCH, R. J., AMBESI, A., LINDENMAYER, G. E. & BLAUSTEIN, M. P. (1992). Presynaptic localization of sodium/calcium exchangers in neuromuscular preparations. *Journal of Neuroscience* **12**, 4898–4904.

MCGRAW, C. F., SOMLYO, A. V. & BLAUSTEIN, M. P. (1980). Localization of calcium in presynaptic nerve terminals. *Journal of Cell Biology* **85**, 228–241.

MARLIER, L. N. J.-L., ZHENG, T., TANG, J. & GRAYSON, D. R. (1993). Regional distribution in the rat central nervous system of a mRNA encoding a portion of the cardiac sodium/calcium exchanger isolated from cerebellar granule neurons. *Molecular Brain Research* **20**, 21–39.

MATSUOKA, S. & HILGEMANN, D. W. (1992). Steady-state and dynamic properties of cardiac sodium–calcium exchange. Ion and voltage dependencies of the transport cycle. *Journal of General Physiology* **100**, 963–1001.

MILANICK, M. A. (1991). Na–Ca exchange: evidence against a ping-pong mechanism and against a Ca pool in ferret red blood cells. *American Journal of Physiology* **261**, C185–193.

MIURA, Y. & KIMURA, J. (1989). Sodium–calcium exchange current. Dependence on internal Ca and Na and competitive binding of external Na and Ca. *Journal of General Physiology* **93**, 1129–1145.

NACHSHEN, D. A. (1985). The early time course of potassium-stimulated calcium uptake in presynaptic nerve terminals from isolated rat brains. *Journal of Physiology* **361**, 251–268.

NACHSHEN, D. A. & BLAUSTEIN, M. P. (1979). The effects of some organic 'calcium antagonists' on calcium influx in presynaptic nerve terminals. *Molecular Pharmacology* **16**, 579–586.

NAHORSKI, S. R. (1988). Inositol polyphosphates and neuronal calcium homeostasis. *Trends in Neurosciences* **11**, 444–448.

NIGGLI, E. & LEDERER, W. J. (1993). Activation of Na–Ca exchange current by photolysis of 'caged calcium'. *Biophysical Journal* **65**, 882–891.

RAITERI, M., BONANNO, G., MARCHI, M. & MAURA, G. (1984). Is there a functional linkage between neurotransmitter uptake mechanisms and presynaptic receptors? *Journal of Pharmacology and Experimental Therapeutics* **231**, 671–677.

RASGADO-FLORES, H. & BLAUSTEIN, M. P. (1987). ATP-dependent regulation of cytoplasmic free calcium in nerve terminals. *American Journal of Physiology* **252**, C588–594.

RASGADO-FLORES, H., SANTIAGO, E. M. & BLAUSTEIN, M. P. (1989). Kinetics and stoichiometry of coupled Na efflux and Ca influx (Na^+–Ca^{2+} exchange) in barnacle muscle cells. *Journal of General Physiology* **93**, 1219–1241.

REEVES, J. P. & SUTKO, J. L. (1983). Competitive interactions of sodium and calcium with the sodium–calcium exchange system of cardiac sarcolemmal vesicles. *Journal of Biological Chemistry* **258**, 3178–3182.

SANCHEZ-ARMASS, S. & BLAUSTEIN, M. P. (1987). Role of Na^+–Ca^{2+} exchange in the regulation of intracellular Ca^{2+} in nerve terminals. *American Journal of Physiology* **252**, C595–603.

SCHWEITZER, E. S. & BLAUSTEIN, M. P. (1980). Calcium buffering in presynaptic nerve terminals. Free calcium levels measured with arsenazo III. *Biochimica Biophysica Acta* **600**, 912–921.

SEGEL, I. H. (1976). *Biochemical Calculations*, 2nd edn. John Wiley and Sons, New York.

SMITH, S. J. & AUGUSTINE, G. J. (1988). Calcium ions, active zones and synaptic transmitter release. *Trends in Neurosciences* **11**, 458–464.

WERTH, J. L. & THAYER, S. A. (1994). Mitochondria buffer physiological calcium loads in cultured rat dorsal root ganglion neurons. *Journal of Neuroscience* **14**, 348–356.

YASUI, K. & KIMURA, J. (1990). Is potassium co-transported by the cardiac Na–Ca exchange? *Pflügers Archiv* **415**, 513–515.

YIP, R. K., BLAUSTEIN, M. P. & PHILIPSON, K. D. (1992). Immunologic identification of Na^+–Ca^{2+} exchange protein in rat brain synaptic plasma membrane. *Neuroscience Letters* **135**, 123–126.

Acknowledgements

We thank Professor M. Raiteri for support and encouragement. These studies were supported by a research grant from the National Institutes of Health (NS-16106). G.F. was funded, in part, by a stipend from the Ministero dell Universit e dell Ricerca Scientifica e Technologica (MURST), Rome, Italy.

Author's present address

Dr G. Fontana: Istituto di Farmacologia e Farmacognosia, Universit di Genova, Viale Cembrano 4, Genova 16148, Italy.

Received 10 June 1994; accepted 22 November 1994.